

Acetylcholine induces voltage-independent increase of cytosolic calcium in mouse myotubes

(acetylcholine receptors/ Ca^{2+} transients/inositol 1,4,5-trisphosphate)

ALDO GIOVANELLI*[†], FRANCESCA GRASSI*[†], ELISABETTA MATTEI*[‡], ANNA M. MILEO*,
AND FABRIZIO EUSEBI*^{†§}

*Laboratorio di Biofisica, Centro della Ricerca Sperimentale Istituto Regina Elena, Via delle Messi d'Oro 156, I-00158 Rome, Italy; [†]Dipartimento di Medicina Sperimentale, Università dell'Aquila, I-67100 L'Aquila, Italy; and [‡]Istituto di Tecnologie Biomediche, Consiglio Nazionale delle Ricerche, via Morgagni 30/e, I-00161 Rome, Italy

Communicated by Ricardo Miledi, August 12, 1991 (received for review May 16, 1991)

ABSTRACT Electrophysiological, biochemical, and Ca^{2+} imaging studies of cultured mouse myotubes were used to investigate whether the neurotransmitter acetylcholine causes an increase in intracellular Ca^{2+} concentration ($[\text{Ca}^{2+}]_i$) through activation of a second messenger system. Bath applications of acetylcholine to myotubes (i) elicited a significant membrane current even in a Na^+ -free Ca^{2+} medium, when the current was carried mainly by calcium ions; (ii) caused a rapid and transient cytosolic accumulation of inositol 1,4,5-trisphosphate; (iii) evoked a conspicuous α -bungarotoxin-sensitive long-lasting $[\text{Ca}^{2+}]_i$ enhancement even in the presence of Cd^{2+} ; and (iv) transiently increased $[\text{Ca}^{2+}]_i$ when cells were equilibrated in a Ca^{2+} -free atropine-containing medium. We propose that, in addition to opening ion channels, the nicotinic action of acetylcholine on the muscle cell membrane increases $[\text{Ca}^{2+}]_i$ through activation of the inositol 1,4,5-trisphosphate second messenger system and mobilization of Ca^{2+} from intracellular stores.

It has been recently reported that the neurotransmitters acetylcholine (ACh) in muscle cells and glutamate in nerve cells and oocytes stimulate the turnover of phosphatidylinositol (PtdIns) (1–4). This event has been shown to evoke a conspicuous Ca^{2+} release from specialized intracellular stores (5, 6). However, the question remains whether the related PtdIns stimulation is derived from the coupling of the transmitter receptor to the PtdIns second messenger system (7) or is a consequence of transmitter-induced increase in cell membrane permeability to Ca^{2+} (8).

To examine this question, we have studied inositol phosphate metabolism and determined the cytosolic calcium level in mouse aneural cultured myotubes exposed to ACh. Here we present evidence that the nicotinic action of ACh induces an elevation of intracellular Ca^{2+} concentration ($[\text{Ca}^{2+}]_i$) due to ACh-induced Ca^{2+} entry and release of Ca^{2+} from intracellular stores, which is, at least in part, mediated by the inositol trisphosphate (InsP_3) pathway.

MATERIALS AND METHODS

Cell Culture. The mouse myogenic cell line C2/C12 (9) was grown (37°C) in Dulbecco's modified Eagle's medium (DMEM) supplemented with 20% (vol/vol) fetal calf serum. Differentiated myotubes were obtained by changing the medium at day 3 (70% confluency) to DMEM supplemented with 2% (vol/vol) horse serum. In our experimental conditions, 4- to 6-day-old myotubes do not contract either spontaneously or after transmitter stimulation.

The publication costs of this article were defrayed in part by page charge payment. This article must therefore be hereby marked "advertisement" in accordance with 18 U.S.C. §1734 solely to indicate this fact.

Electrophysiology. Experiments were performed at room temperature (23–25°C) on 2-day-old replicating satellite cells or on 4- to 6-day-old cultured myotubes. Membrane currents were recorded using the whole-cell configuration of the patch-clamp method as described (10) and digitized at 100 Hz. Cells were equilibrated in a normal external solution (NES) containing 140 mM NaCl, 2.8 mM KCl, 2 mM CaCl_2 , 2 mM MgCl_2 , 10 mM glucose, and 10 mM Hepes-NaOH (pH 7.3). Ca^{2+} -free medium was obtained by replacing Ca^{2+} with Mg^{2+} (4 mM). High- Ca^{2+} Na^+ -free medium contained 20 mM CaCl_2 , 2.8 mM KCl, 220 mM sucrose, and 5 mM Hepes-CsOH (pH 7.3) (280 milliosmolar). The whole-cell recording pipette solution consisted of 120 mM CsCl, 20 mM tetraethylammonium chloride, 2 mM MgCl_2 , 1 mM CaCl_2 , 11 mM EGTA, 2 mM ATP, and 10 mM Hepes-CsOH (pH 7.3). Cells were continuously superfused with saline solutions applied by a gravity-driven perfusion system. Two distinct perfusion lines contained either the external solution alone or with 10–30 μM ACh. Solutions were applied individually and in succession through a double-barreled pipette with a tip diameter of 80–100 μm positioned $\approx 200 \mu\text{m}$ from the cell, such that the whole myotube was superfused.

Determination of PtdIns Turnover. PtdIns turnover in the myotubes was determined by established procedures (11). Differentiated 5-day-old myotubes were incubated with *myo*-[2-³H]inositol (Amersham; 5 $\mu\text{Ci}/\text{ml}$; 1 Ci = 37 GBq) and after 24 hr rinsed three times at 37°C with fresh serum-free DMEM. LiCl (20 mM) was added to the medium 20 min before starting treatments. At the end of the experiments, the medium was rapidly removed and myotubes were exposed to ice-cold trichloroacetic acid [10% (wt/vol)] to terminate the reaction. Samples were then transferred to ice for 30 min and processed as described (1, 2). Trichloroacetic acid extracts were centrifuged at 700 $\times g$ for 10 min and the supernatants were extracted five times with water-saturated diethyl ether, neutralized with 1M Tris-HCl (pH 8.8), and freeze-dried. Lyophilized samples were resuspended in a small volume of water and equal amounts of radioactivity were loaded on an HPLC apparatus (LKB). The chromatography was performed on a Whatman Partisil 10 SAX anion-exchange analytical column (25 cm \times 0.46 cm). Samples were filtered through a 0.22- μm filter (Dyna Gard, Microgon, CA) before loading on the column. Unlabeled nucleotide markers (AMP, ADP, ATP, GMP, GDP, and GTP; each at 70 mM) were routinely added as internal standards and their elution was

Abbreviations: ACh, acetylcholine; nAChR, nicotinic ACh receptor; InsP , InsP_2 , etc., inositol monophosphate, inositol biphosphate, etc.; $\text{Ins}(1,4,5)\text{P}_3$, inositol 1,4,5-trisphosphate; PtdIns, phosphatidylinositol; $[\text{Ca}^{2+}]_i$, intracellular Ca^{2+} concentration; α -BuTX, α -bungarotoxin.

§To whom reprint requests should be addressed at: Laboratorio di Biofisica, Centro della Ricerca Sperimentale Istituto Regina Elena, Via delle Messi d'Oro 156, I-00158 Rome, Italy.

evaluated by absorption at 254 nm. Inositol 1,4,5-[5-³²P]triphosphate (New England Nuclear) was added to identify the position of inositol 1,4,5-trisphosphate [Ins(1,4,5)P₃]. Separation of inositol phosphates was achieved using a step gradient from 100% water to 1.7 M ammonium formate buffered to pH 3.7 with orthophosphoric acid (11). Ninety-four samples (0.24 ml) were collected and radioactivity was measured in a Beckman LS-1800 counter, after the addition of 5 ml of scintillant. The solutions used for experiments had the same composition as those used for electrophysiology.

Ca²⁺ Imaging. Fluorescence measurements and Ca²⁺ imaging analysis were performed as described (12). Briefly, myotubes were loaded at 37°C in an O₂/CO₂ incubator with 2.5 μM fura-2 tetrakis(acetoxymethyl) ester (AM) (Calbiochem) in DMEM (Flow Laboratories) with 2% heat-inactivated horse serum (GIBCO) for 30 min. The fura-2 AM stock solution (1 mM in dimethyl sulfoxide) was stored at -20°C. After loading, the fura-2 solution was replaced by NES. The best signal was obtained when the fura-2 AM was allowed to deesterify for 5–20 min. This regime produced homogeneously labeled myotubes. Neutral density filters of 1.0–1.5 OD units were used to protect the myotube from phototoxicity and bleaching. The fluorescence images were acquired from an inverted microscope (Diaphot; Nikon) equipped with a Hg UV lamp and with a high-sensitivity camera (extended ISIS-M; Photonic Science, U.K.). The Magiscan image processing unit (Joyce-Loebl) was used for image capture and analysis. The fluorescence intensity at 340 and 380 nm was verified on an oscilloscope before starting data acquisition. The ratios *R* of fluorescence intensities at 340 and 380 nm ($R = I_{340}/I_{380}$) were calculated after subtracting background fluorescence values from a cell-free region of the coverslip. *R* values were converted to [Ca²⁺]_i values by the calibration curve (13):

$$[\text{Ca}^{2+}]_i = K_d \beta (R - R_{\min}) / (R_{\max} - R),$$

where *K_d*, the dissociation constant of fura 2, is 225 nM; β, the calibration constant defined as *I*₃₈₀ (at *R*_{min})/*I*₃₄₀ (at *R*_{max}) in our system is 4. The *R*_{min} of 0.3 and *R*_{max} of 2.125 were measured and averaged from six experiments in cells treated in sequence with 5 μM ionomycin (Calbiochem) and 20 mM EGTA (Sigma). For determinations of [Ca²⁺]_i, the calibration scale was properly used to get maximum resolution and to avoid saturation. During imaging sessions, myotubes were continuously superfused with the control solution (NES) using the above described perfusion system. All images were collected at ×1000 magnification.

RESULTS

AcCho-Induced Membrane Currents. Whole-cell patch-clamped multinucleate myotubes responded to AcCho with a long-lasting current that had an amplitude of 1–5 nA at a membrane holding potential of -70 mV (Fig. 1). The current was irreversibly blocked by the nicotinic antagonist α-bungarotoxin (α-BuTX, 10 nM) and was unaffected by the muscarinic antagonist atropine (10 μM). A similar slowly decaying current was also observed in the presence of either high-Ca²⁺ Na⁺-free sucrose medium or Ca²⁺-free medium (Fig. 1). Mononucleate satellite cells were also responsive to AcCho but the currents elicited were smaller in size (70–500 pA) and decayed faster when compared to those in multinucleate myotubes (data not shown). In multinucleate myotubes, voltage steps to 0–20 mV activated Ca²⁺ currents that were blocked by Cd²⁺, whereas these currents failed to occur in most replicating satellite cells (data not shown).

PtdIns Turnover. It has previously been shown that the nicotinic action of AcCho on the chicken myotube membrane stimulates the release of inositol monophosphate (InsP) (1,

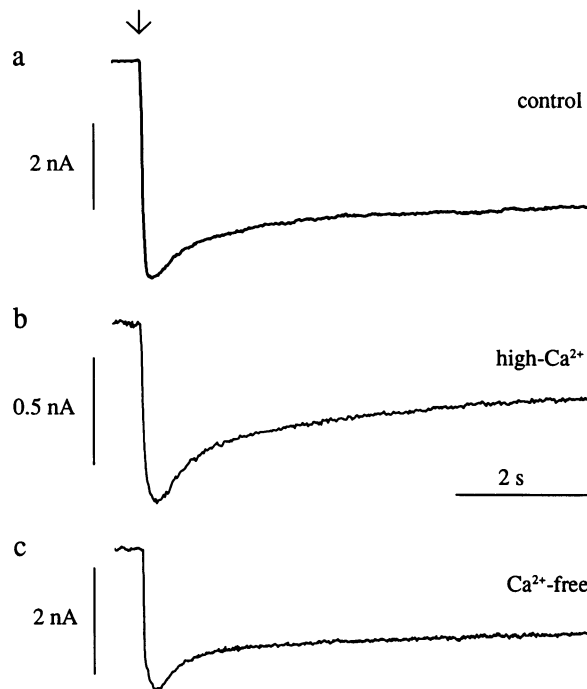


FIG. 1. Typical AcCho-activated currents in 5-day-old myotubes. (a) Response to 20 μM AcCho in a myotube equilibrated in NES. (b) Response of a myotube bathed in high Ca²⁺ Na⁺-free medium and superfused with 20 μM AcCho dissolved in the same solution. (c) A different myotube equilibrated in Ca²⁺-free medium and superfused with 20 μM AcCho in the same medium. Experiments were done at room temperature (24°C). Arrow indicates onset of AcCho application, which was continued beyond the end of the traces. Notice smaller amplitude and faster recovery of the current (b) carried only by Ca²⁺ (in Na⁺-free medium). The three myotubes were clamped at -70 mV.

2). To investigate whether the AcCho-induced accumulation of InsP is a degradation product of InsP₃ formed during nicotinic AcCho receptor (nAcChoR) activation, the metabolism of inositol phosphates was studied in 5-day-old mouse myotubes exposed to AcCho (10–30 μM).

In untreated myotubes there was a marked basal level of InsP₃, inositol tetrakisphosphate (InsP₄), inositol bisphosphate (InsP₂), and InsP. Within the first 5 s of AcCho treatment, InsP₃ increased by 1.3- to 2.7-fold and then rapidly decreased (Fig. 2). In contrast, both InsP and InsP₂, which are products of InsP₃ degradation (5, 6), increased to ≈2-fold within 60 s after AcCho application and continued to increase thereafter (data not shown).

To block voltage-dependent Ca²⁺ channels that are activated by transmitter-induced depolarization (15), some experiments were performed in the presence of Cd²⁺. A Cd²⁺ concentration of 200 μM was chosen, since this was sufficient to fully block the voltage-activated Ca²⁺ channels in myotubes (for an example, see Fig. 3b). The basal PtdIns hydrolysis was higher in the presence of Cd²⁺ than in the standard medium. This was probably due to inhibition of InsP₃ phosphatase (16), possibly with Cd²⁺-induced stimulation of PtdIns turnover (17). Nevertheless, PtdIns turnover was further stimulated by AcCho in Cd²⁺-treated myotubes. For instance in three experiments, the maximal InsP₃ increase was ≈1.7-fold, indicating that the Ca²⁺ influx due to membrane depolarization is not substantially important for the accumulation of InsP₃.

To investigate whether Ca²⁺ entry through the nAcChoR channels (18, 19) could play a role on the PtdIns hydrolysis, experiments were carried out in myotubes equilibrated in Ca²⁺-free medium. In these myotubes the basal PtdIns me-

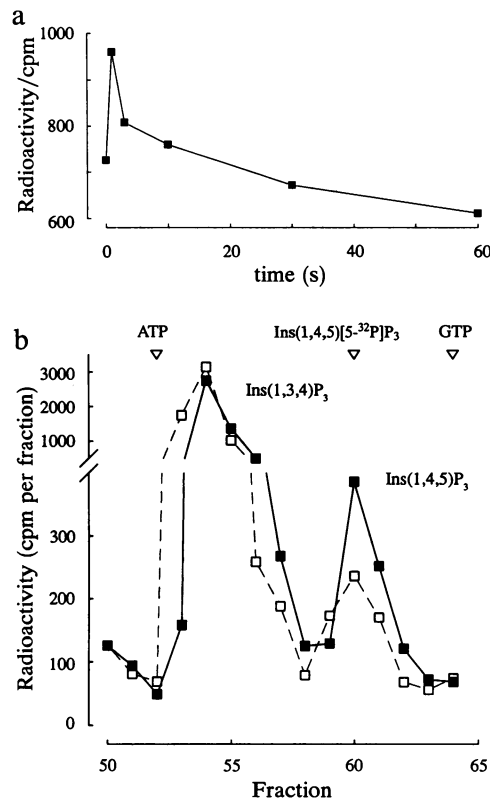


FIG. 2. Typical accumulation of InsP_3 in AcCho-stimulated myotubes. (a) Cells were exposed to $30 \mu\text{M}$ AcCho in serum-free DMEM. Basal values were plotted at zero time. Each point represents the average of three dishes, each assayed in duplicate. The experiment was performed at room temperature (23°C). The time of exposure to AcCho vs. the total radioactivity in InsP_3 fractions in cpm is plotted. Note the peak of $\text{Ins}(1,4,5)\text{P}_3$ after 1 s and subsal values after 20 s of AcCho application (see ref. 14). In this experiment, InsP values rose to 160% of the control after 60 s of AcCho application. (b) HPLC elution pattern of InsP_3 after 1 s of AcCho application. Same experiment as a. [³H]inositol-prelabeled myotubes were exposed to $30 \mu\text{M}$ AcCho for 1 s. Equal amounts of radioactivity (5×10^5 cpm) from control and treated samples were separated by HPLC. Fractions lower than 50 and higher than 64, which include peaks of free inositol, glycerophosphoinositol, InsP , InsP_2 , and InsP_4 were omitted in the figure. InsP_3 -containing fractions were collected between 45 and 50% (vol/vol) ammonium formate. Open triangles, markers; open squares, control myotubes; solid squares, AcCho-treated myotubes. Note a 1.6-fold increase in $\text{Ins}(1,4,5)\text{P}_3$.

tabolism was strongly reduced. Nonetheless, in two experiments a 1.3-fold increase in $\text{Ins}(1,4,5)\text{P}_3$ was detected after a 3-s AcCho application. In three other experiments, InsP_3 accumulation was not detectable after a 15-s AcCho application. These results (i) indicate that the presence of Ca^{2+} in the external solution was very important for both basal metabolism and activation of InsP_3 system in myotubes and (ii) suggest that a stimulation of PtdIns turnover, even if weak, was still present in Ca^{2+} -free medium.

AcCho-Induced Increase of $[\text{Ca}^{2+}]_i$. Ca^{2+} imaging techniques were applied to 5-day-old myotubes to investigate whether AcCho causes an increase in $[\text{Ca}^{2+}]_i$. During brief applications of AcCho (10 – $30 \mu\text{M}$), $[\text{Ca}^{2+}]_i$ rose rapidly to ≈ 20 -fold its resting level and fell promptly toward basal levels after its removal but, in the continuous presence of AcCho, the $[\text{Ca}^{2+}]_i$ decreased only slowly to its original value (Fig. 3a). The AcCho-induced increase in $[\text{Ca}^{2+}]_i$ was most probably due to activation of the nAcChoR since the Ca^{2+} response to AcCho showed a half-decay time (Table 1) similar to that of the AcCho current response (Fig. 1 and ref.

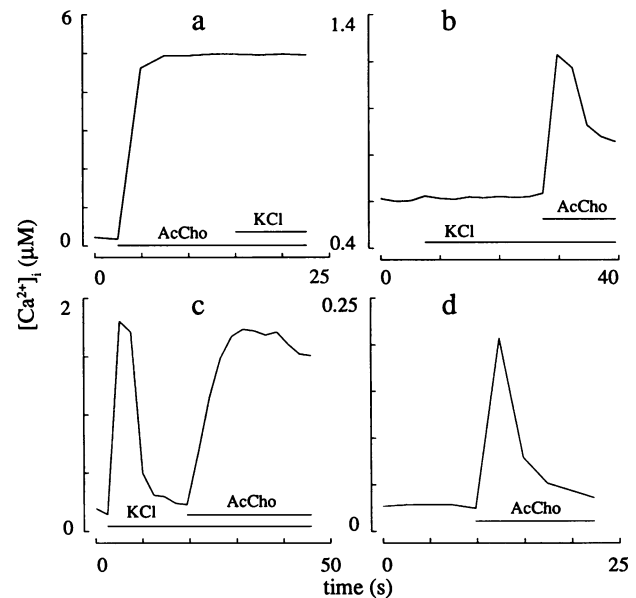


FIG. 3. AcCho-evoked Ca^{2+} transients in 5-day-old myotubes. The traces represent the time course of responses from four myotubes. Ca^{2+} signals were averaged on the whole cell. Initially, the myotubes in a–c were superfused with NES. AcCho and/or Ca^{2+} -containing K^+ medium were applied as indicated. For these experiments, a three-barreled perfusion pipette was used. (a) Myotube superfused with NES and then successively exposed to NES containing $30 \mu\text{M}$ AcCho and to isotonic K^+ medium containing AcCho. (b) Myotube superfused with NES containing $200 \mu\text{M}$ Cd^{2+} and then successively exposed to isotonic K^+ medium containing $200 \mu\text{M}$ Cd^{2+} and to $30 \mu\text{M}$ AcCho in the same medium. Note the higher basal level of resting $[\text{Ca}^{2+}]_i$ due to the presence of Cd^{2+} . (c) Myotube superfused with isotonic K^+ medium and then with the medium plus $30 \mu\text{M}$ AcCho. (d) Myotube superfused with Ca^{2+} -free medium containing $200 \mu\text{M}$ Cd^{2+} and $10 \mu\text{M}$ atropine, and then with $30 \mu\text{M}$ AcCho in the same medium. Note the low basal $[\text{Ca}^{2+}]_i$. Horizontal bars, superfusion of modified medium. These experiments were performed at room temperature (24°C).

20), and it was completely blocked by 10 nM α -BuTX (Table 1). In addition this response was not affected by $10 \mu\text{M}$ atropine (two experiments, data not shown).

Cells exhibited considerable variability in the magnitude of the response to AcCho within the same culture and over time in culture. For instance, in a culture the increase in $[\text{Ca}^{2+}]_i$ ranged from 2- to 5-fold in 2-day-old mononucleate satellite cells ($n = 14$) and from 16- to 35-fold in 3-day-old multinucleate myotubes ($n = 8$). This could reflect variations in nAcChoR density since, as seen before, a large variability was also observed within the AcCho-elicited whole-cell currents in the same culture and during myogenesis (unpublished observations).

To block the depolarization-induced Ca^{2+} influx, experiments were performed in myotubes treated with $200 \mu\text{M}$ Cd^{2+} . Myotubes exposed to Cd^{2+} exhibited higher levels of cytosolic Ca^{2+} than control myotubes (Table 1), again probably due to Cd^{2+} -induced increases in PtdIns hydrolysis. In these myotubes, exposure to 30 mM K^+ did not alter the cytosolic Ca^{2+} level, indicating that the depolarization-activated Ca^{2+} channels had been blocked by Cd^{2+} . In contrast, during AcCho application a considerable increase in $[\text{Ca}^{2+}]_i$ was observed in the presence of Cd^{2+} , but the Ca^{2+} -transient had a smaller amplitude and faster decay when compared with that in the standard medium (Fig. 3b and Table 1).

In other experiments the myotube was exposed to isotonic K^+ medium and after the K^+ -induced Ca^{2+} transient had subsided, AcCho was added to the high K^+ medium. A representative example illustrated in Fig. 3c shows that AcCho still elicited a well-maintained increase in $[\text{Ca}^{2+}]_i$. In contrast,

Table 1. Effects of superfusion of 5-day-old fura-2-loaded myotubes with 30 μM AcCho and with 30 mM potassium

Medium	Resting $[\text{Ca}^{2+}]_i$, μM	Peak $[\text{Ca}^{2+}]_i$, μM	Half-decay time, s	N
AcCho				
NES	0.17 ± 0.05	3.79 ± 0.24	>60	16
K ⁺ -ES	0.29 ± 0.08	1.37 ± 0.18	16.2 ± 2.6	13
Cd ²⁺ -ES	0.69 ± 0.04	3.89 ± 0.27	5.1 ± 0.6	10
Ca ²⁺ -free ES	0.05 ± 0.01	0.21 ± 0.02	1.9 ± 0.2	16
Potassium				
NES	0.14 ± 0.04	1.84 ± 0.21	1.7 ± 0.3	10
AcCho-ES	0.15 ± 0.04	0.16 ± 0.02	—	8
Cd ²⁺ -ES	0.52 ± 0.12	0.62 ± 0.15	—	5
Ca ²⁺ -free ES	0.10 ± 0.02	0.11 ± 0.03	—	4

ES, external solution; K⁺-ES, isotonic K⁺ medium, with K⁺ substituted for Na⁺; Cd²⁺-ES, 200 μM Cd²⁺ in NES; AcCho-ES, AcCho in NES; Ca²⁺-free ES, Ca²⁺-free NES containing 10 μM atropine, 200 μM Cd²⁺, and 2 mM EGTA. Values represent mean \pm SEM. Resting $[\text{Ca}^{2+}]_i$, basal level of cytosolic Ca²⁺; peak $[\text{Ca}^{2+}]_i$, amplitude of the Ca²⁺ response at the peak. The half-decay time was the time required for the signal to decay from the peak value to half the peak value.

the exposure to K⁺ during the maintained action of AcCho did not cause a further increase in $[\text{Ca}^{2+}]_i$ (Fig. 3a and Table 1), probably because of inactivation of the voltage-dependent Ca²⁺ channels after depolarization by AcCho. Since during prefusion myogenesis satellite cells may lack voltage-dependent currents, one experiment was performed on 2-day-old satellite cells that did not exhibit voltage-dependent Ca²⁺ currents when electrically stimulated. These cells were nevertheless still responsive to AcCho (data not shown). Thus, with results obtained by exposing cells to either Cd²⁺ or isotonic K⁺ medium, these findings indicate that Ca²⁺ entry through voltage-dependent Ca²⁺ channels provides only a partial contribution to the increase in $[\text{Ca}^{2+}]_i$ elicited by AcCho.

Another potential means of elevating $[\text{Ca}^{2+}]_i$ is Ca²⁺ entry through active nAcChoR channels (18, 19). Thus, experiments were also carried out with myotubes bathed in EGTA-containing Ca²⁺-free medium. In these conditions, the basal $[\text{Ca}^{2+}]_i$ concentration was very low, and it remained below normal values even in the presence of Cd²⁺ (see Table 1). These myotubes responded to AcCho giving a fast transient with a peak amplitude of $0.24 \pm 0.06 \mu\text{M}$ (4-fold increase; *n*

= 10). The $[\text{Ca}^{2+}]_i$ increase was not substantially modified by preincubating with atropine and Cd²⁺ in Ca²⁺-free medium (Fig. 3d and Table 1) but was abolished by α -BuTX (two myotubes, data not shown). In a few myotubes, the $[\text{Ca}^{2+}]_i$ increase was followed by a decrease in $[\text{Ca}^{2+}]_i$ below basal levels. Since under these conditions the increase of $[\text{Ca}^{2+}]_i$ cannot be derived from a Ca²⁺ entry, these results suggest that the observed AcCho responses of muscle cells exposed to Ca²⁺-free medium were substantially due to the mobilization of Ca²⁺ from internal stores. This is supported by the spatial distribution of the Ca²⁺ signals that were localized in myotubes bathed in a Ca²⁺-free medium but had a more uniform distribution in muscle cells exposed to AcCho in the standard medium. Such a difference is illustrated in Fig. 4, which gives a representative example of pseudocolor images of $[\text{Ca}^{2+}]_i$ in myotubes treated with AcCho in either NES or Ca²⁺-free medium.

DISCUSSION

We have shown that in mouse myotubes activation of nAcChoRs elicits a long-lasting increase in $[\text{Ca}^{2+}]_i$. Large Ca²⁺ responses to AcCho still develop when Ca²⁺ entry across

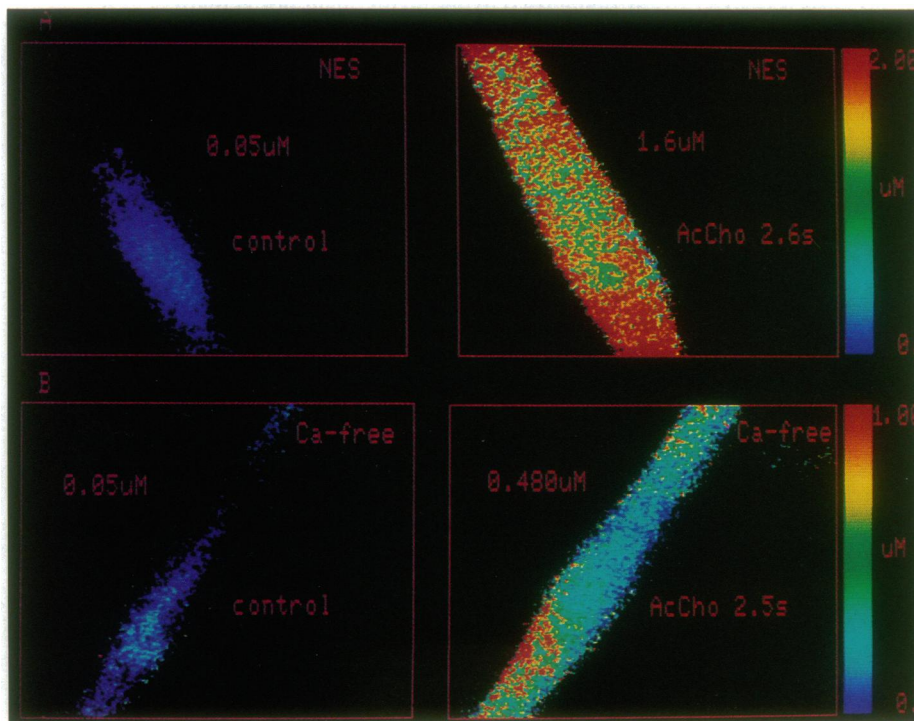


FIG. 4. Spatial organization of calcium signaling in 5-day-old myotubes. $[\text{Ca}^{2+}]_i$ levels were determined by image analysis of fura-2 signals. Color bars by the panels give the Ca²⁺ concentration in the 256 pseudocolor level scale. The vertical length of the frame corresponds to 100 μm . The reported values of $[\text{Ca}^{2+}]_i$ (in μM) are obtained by averaging all pixels in the cell. (A) Distributed AcCho-evoked $[\text{Ca}^{2+}]_i$ increase in NES. (B) Localized $[\text{Ca}^{2+}]_i$ increase in Ca²⁺-free medium containing 100 nM atropine, 200 μM Cd²⁺, and 2 mM EGTA. Notice the different pseudocolor scale for A and B.

voltage-dependent channels is blocked. The Ca^{2+} transient becomes smaller in size and decays faster when Ca^{2+} entry through nAcChoR channels is also inhibited, indicating that the main component of Ca^{2+} response is due to Ca^{2+} entry through active nAcChoR channels and through voltage-dependent channels. Nevertheless, in the Ca^{2+} -free medium, there is still a residual transient increase in $[\text{Ca}^{2+}]_i$ that appears to be due to the release of cytosolic Ca^{2+} from intracellular stores. A candidate messenger for this AcCho action is $\text{Ins}(1,4,5)\text{P}_3$, which increases in concentration in myotubes after AcCho treatment and is known to mobilize Ca^{2+} from intracellular compartments (5, 6). This might even be a general action of excitatory neurotransmitters on their target cells, since glutamate is capable of stimulating PtdIns turnover (3, 21, 22) and elevating $[\text{Ca}^{2+}]_i$ in neurons equilibrated in Ca^{2+} -free medium (23). However, it remains to be established whether the $[\text{Ca}^{2+}]_i$ increase detected in a Ca^{2+} -free medium is due only to InsP_3 accumulation or to other signaling pathways as well.

Interestingly, the accumulation of InsP_3 suggests also a cytosolic elevation of diacylglycerol (5, 6), the physiological stimulator of the protein kinase C (24). It has been shown that protein kinase C activity, as well as an increase in $[\text{Ca}^{2+}]_i$, may be involved in nAcChoR desensitization (25, 26). Thus AcCho might activate a cascade process leading to the desensitization of its own nAcChoR through an $[\text{Ca}^{2+}]_i$ increase and protein kinase C activation.

It is now generally accepted that two classes of receptors are associated with the action of neurotransmitters at synapses: ionotropic or ligand-gated receptor-ion channel complexes and guanine nucleotide binding (G) protein-coupled receptors (27). Upon binding to the neurotransmitter, ionotropic receptors directly open channels and ions flow across the membrane. The interaction of transmitters with metabotropic receptors causes activation of G proteins, which either directly couple to ion channels or regulate channels by second messenger systems. The present data suggest that the ionotropic class of receptors might also couple to second messenger systems.

At present, however, it remains possible that, with activation of nAcChoRs, AcCho also activates an uncharacterized class of metabotropic receptors. These receptors would have to be insensitive to atropine, sensitive to α -BuTX, and coupled to the PtdIns system.

We are grateful to Dr. Ricardo Miledi for advice and helpful suggestions during this work. We thank Drs. Miledi and Richard M. Woodward for critical reading of the manuscript. This work was partially supported by a grant from FIDIA, by a grant from Ministero Universita', Ricerca Scientifica e Tecnologica, and by a grant from Telethon.

1. Adamo, S., Zani, B. M., Nervi, C., Senni, M. I., Molinaro, M. & Eusebi, F. (1985) *FEBS Lett.* **190**, 161–164.
2. Eusebi, F., Grassi, F., Nervi, C., Caporale, C., Adamo, S., Zani, B. M. & Molinaro, M. (1987) *Proc. R. Soc. London Ser. B* **230**, 355–365.
3. Sladeczek, F., Pin, J. P., Recasens, M., Bockaert, J. & Weiss, S. (1985) *Nature (London)* **317**, 717–719.
4. Gundersen, C. B., Miledi, R. & Parker, I. (1984) *Proc. R. Soc. London Ser. B* **221**, 127–143.
5. Berridge, M. (1987) *Annu. Rev. Biochem.* **56**, 159–193.
6. Berridge, M. J. & Irvine, R. F. (1989) *Nature (London)* **341**, 197–205.
7. Meldolesi, J. & Westhead, W. (1989) in *Inositol Lipids in Cell Signalling*, eds. Michell, R. H., Drummond, A. H. & Downes, C. P. (Academic, New York), pp. 311–336.
8. Eberhard, D. A. & Holz, R. W. (1988) *Trends Neurosci.* **11**, 517–520.
9. Yaffe, D. & Saxel, O. (1977) *Nature (London)* **270**, 725–727.
10. Hamill, O. P., Marty, A., Neher, E., Sakmann, B. & Sigworth, F. J. (1981) *Pflügers Arch.* **391**, 85–100.
11. Simpson, C. M. F., Batty, I. H. & Hawthorne, J. N. (1987) *Neurochemistry: A Practical Approach*, eds. Turner, A. J. & Bachelard, H. S. (IRL, Oxford), pp. 193–223.
12. Tsien, R. Y. (1988) *Trends Neurosci.* **11**, 419–424.
13. Grynkiewicz, G., Poenie, M. & Tsien, R. Y. (1985) *J. Biol. Chem.* **260**, 3440–3450.
14. Chilvers, E. R., Challis, R. A. J., Barnes, P. J. & Nahorski, S. R. (1989) *Eur. J. Pharmacol.* **164**, 587–590.
15. Byerly, L. & Hagiwara, S. (1988) in *Calcium and Ion Channel Modulation*, eds. Grinnell, A. D., Armstrong, D. & Jackson, M. B. (Plenum, New York), pp. 3–18.
16. Vergara, J., Tsien, R. Y. & Delay, M. (1985) *Proc. Natl. Acad. Sci. USA* **82**, 6352–6356.
17. Miledi, R., Parker, I. & Woodward, R. M. (1989) *J. Physiol. (London)* **417**, 173–195.
18. Katz, B. & Miledi, R. (1969) *J. Physiol. (London)* **203**, 689–706.
19. Bregestovski, P. D., Miledi, R. & Parker, I. (1979) *Nature (London)* **284**, 560–561.
20. Giovannelli, A., Farini, D., Gauzzi, M. C., Alema, S. & Eusebi, F. (1990) *Cell Signalling* **2**, 347–352.
21. Masu, M., Tanabe, Y., Tsuchida, K., Shigemoto, R. & Nakanishi, S. (1991) *Nature (London)* **349**, 760–765.
22. Houamed, K. M., Kuijper, J. L., Gilbert, T. L., Halderman, B. A., O'Hara, P. J., Mulvihill, E. R., Almers, W. & Hagen, F. S. (1991) *Science* **252**, 1318–1321.
23. Milani, D., Guidolin, L., Facci, L., Pozzan, T., Buso, M., Leon, A. & Skaper, S. D. (1991) *J. Neurosci. Res.* **28**, 434–441.
24. Nishizuka, Y. (1984) *Science* **225**, 1365–1370.
25. Eusebi, F., Molinaro, M. & Zani, B. M. (1985) *J. Cell Biol.* **100**, 1339–1342.
26. Miledi, R. (1980) *Proc. R. Soc. London Ser. B* **209**, 447–452.
27. Strange, P. G. (1988) *Biochem. J.* **249**, 309–318.